

The American Journal of Human Genetics, Volume 95

Supplemental Data

**Mutations in *RAB39B* Cause X-Linked
Intellectual Disability and Early-Onset Parkinson
Disease with α -Synuclein Pathology**

Gabrielle R. Wilson, Joe C.H. Sim, Catriona McLean, Maila Giannandrea, Charles A. Galea, Jessica R. Riseley, Sarah E.M. Stephenson, Elizabeth Fitzpatrick, Stefan A. Haas, Kate Pope, Kirk J. Hogan, Ronald G. Gregg, Catherine J. Bromhead, David S. Wargowski, Christopher H. Lawrence, Paul A. James, Andrew Churchyard, Yujing Gao, Dean G. Phelan, Greta Gillies, Nicholas Salce, Lynn Stanford, Ashley P.L. Marsh, Maria L. Mignogna, Susan J. Hayflick, Richard J. Leventer, Martin B. Delatycki, George D. Mellick, Vera M. Kalscheuer, Patrizia D'Adamo, Melanie Bahlo, David J. Amor, and Paul J. Lockhart

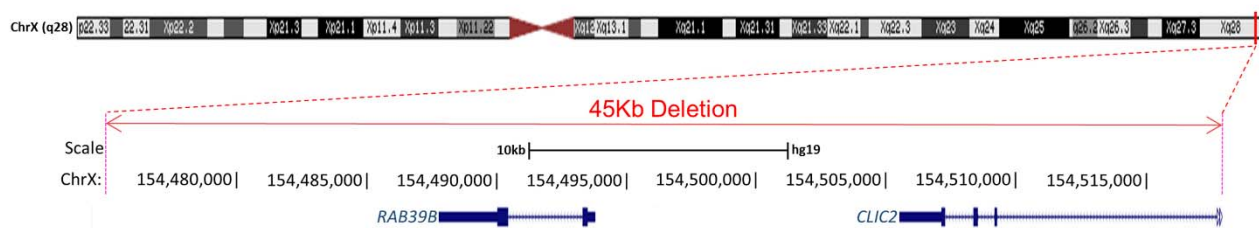
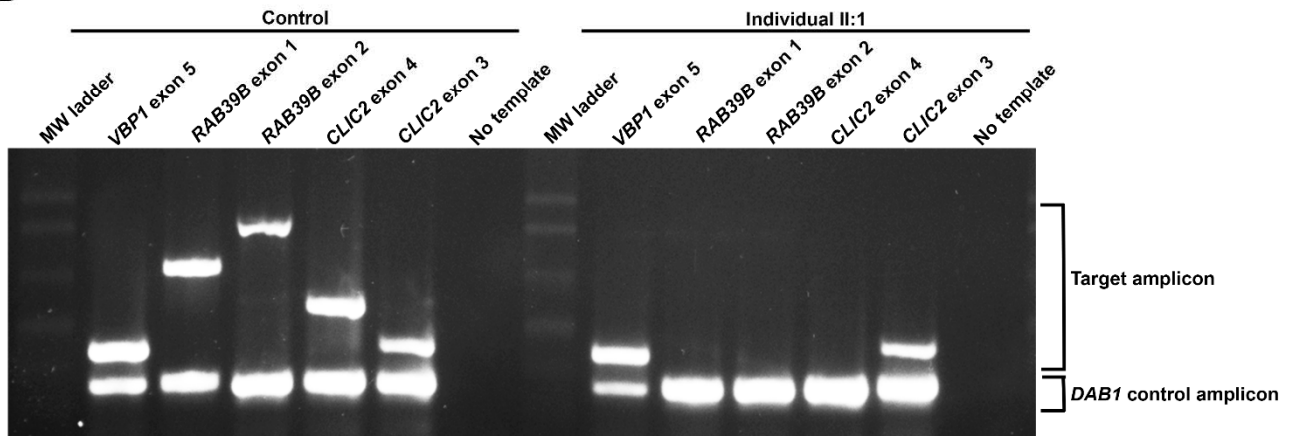
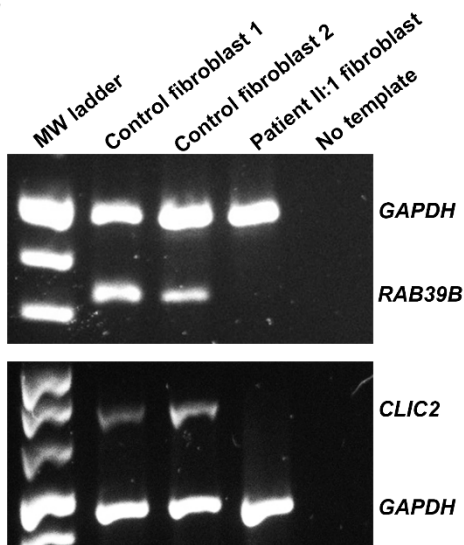
A**B****C**

Figure S1: Confirmation of *RAB39B* deletion in the Australian pedigree.

(A) CNV analysis identified a 45Kb deletion spanning Hg19 ChrX: 154,474,499-154,518,072 that resulted in the deletion of *RAB39B* and the last three exons of *CLIC2*. (B) PCR amplification of *RAB39B* (NG_012626.2) and the surrounding genes, *VBPI* (MIM300133) and *CLIC2* was achieved using primer pairs available on request. A duplex PCR amplifying an independent control gene (*DAB1* [MIM603448]) was performed to confirm the deletion of *RAB39B* and *CLIC2* in the Australian kindred. (C) End-point RT-PCR analysis of fibroblast RNA confirmed the absence of *RAB39B* and *CLIC2* expression in individual II:1. The reactions were duplexed with a primer set targeting *GAPDH* (MIM138400) to confirm template integrity.

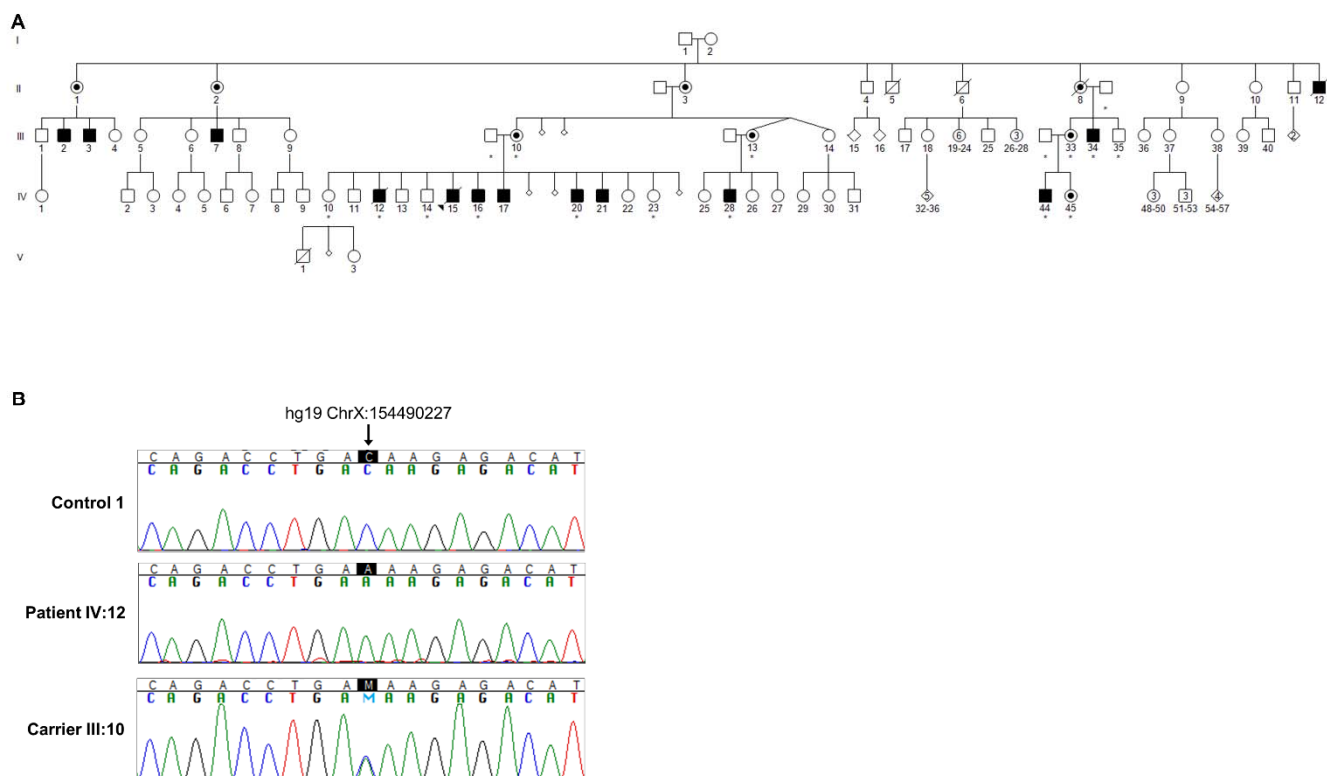


Figure S2: Confirmation of the NM_171998.2: c.503C>A (p.Thr168Lys) mutation in *RAB39B*

(A) Full pedigree of the previously published Wisconsin kindred. Affected males and obligate female carriers are represented by the filled squares and circles with dots respectively. (B) Representative sequence traces confirming the NM_171998.2: c.503C>A, p.Thr168Lys mutation. Sanger sequencing was performed using standard protocols, amplicons were sequenced using Big Dye Terminator v3.1 (Applied Biosystems) and Sequencher software (Gene Codes) was used to analyse sequence traces. * represent individuals with DNA collected.

Figure S3: RAB39B is conserved across evolution

Molecular phylogenetic analysis was performed by the maximum likelihood method based on the Jones-Taylor-Thornton matrix (Molecular Evolution and Genomic Analysis Version 5.2.2). (A) Following whole genome duplication that occurred early in the vertebrate lineage, *Rab39* specified into *Rab39a* and *Rab39b*. Numbers represent the percentage of 1000 bootstraps that reproduced the partition; those with less than 50% replicates have been collapsed. Accession numbers are shown, *determined by TBLATN on genomic sequence, ^partial sequence. (B) Clustal Omega alignment of Rab39a and Rab39b orthologues depicting the conservation of Thr168 and Leu60 in both proteins. Secondary structural motifs for Rab1a (PDB ID: 3TKL) are shown above the alignment where α -helices are represented as cylinders and β -strands as arrows. G1-5 box motifs (defined by the Conserved Domain Database) are shown in bold, and Switch I and Switch II are shaded orange and blue, respectively.

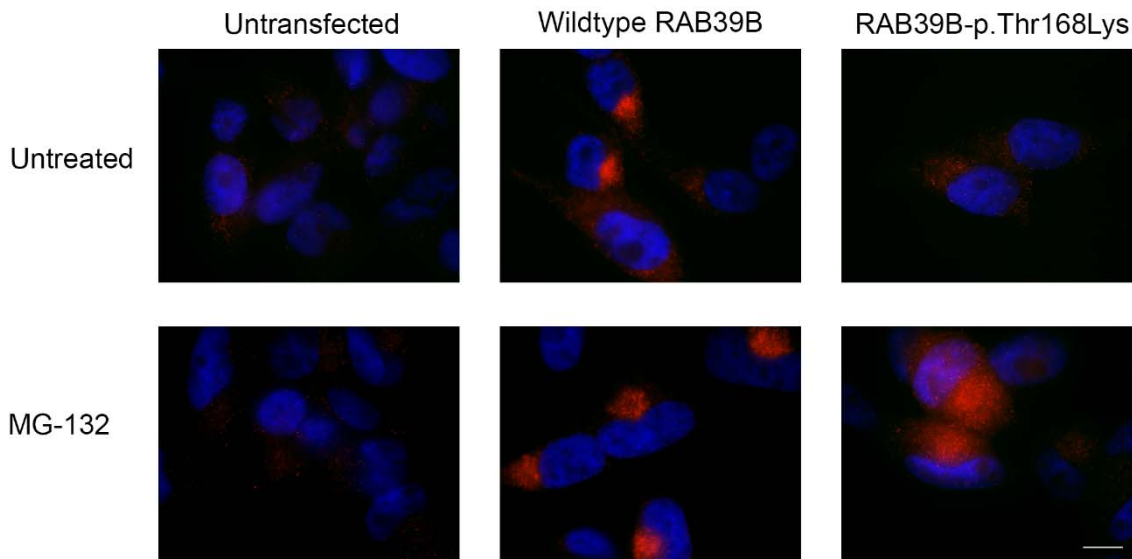


Figure S4: Immunofluorescence analysis suggests that mutant RAB39B-p.Thr168Lys is unstable and degraded by the ubiquitin proteasome system

Immunofluorescence was used to detect endogenous or exogenous RAB39B in BE(2)-M17 neuroblastoma cells, in the absence or presence of 10 μ M MG-132. Endogenous RAB39B appeared as faint but distinct puncta within the cytoplasm. In the absence of MG-132 wildtype RAB39B recombinant protein was highly expressed and distributed throughout the cytoplasm. In contrast, cells expressing mutant RAB39B-p.Thr168Lys demonstrated a low level of immunoreactivity, equivalent to that observed in the untransfected cells. The steady state level of mutant RAB39B-p.Thr168Lys immunoreactivity increased significantly following MG-132 treatment. Scale bar 10 μ m.

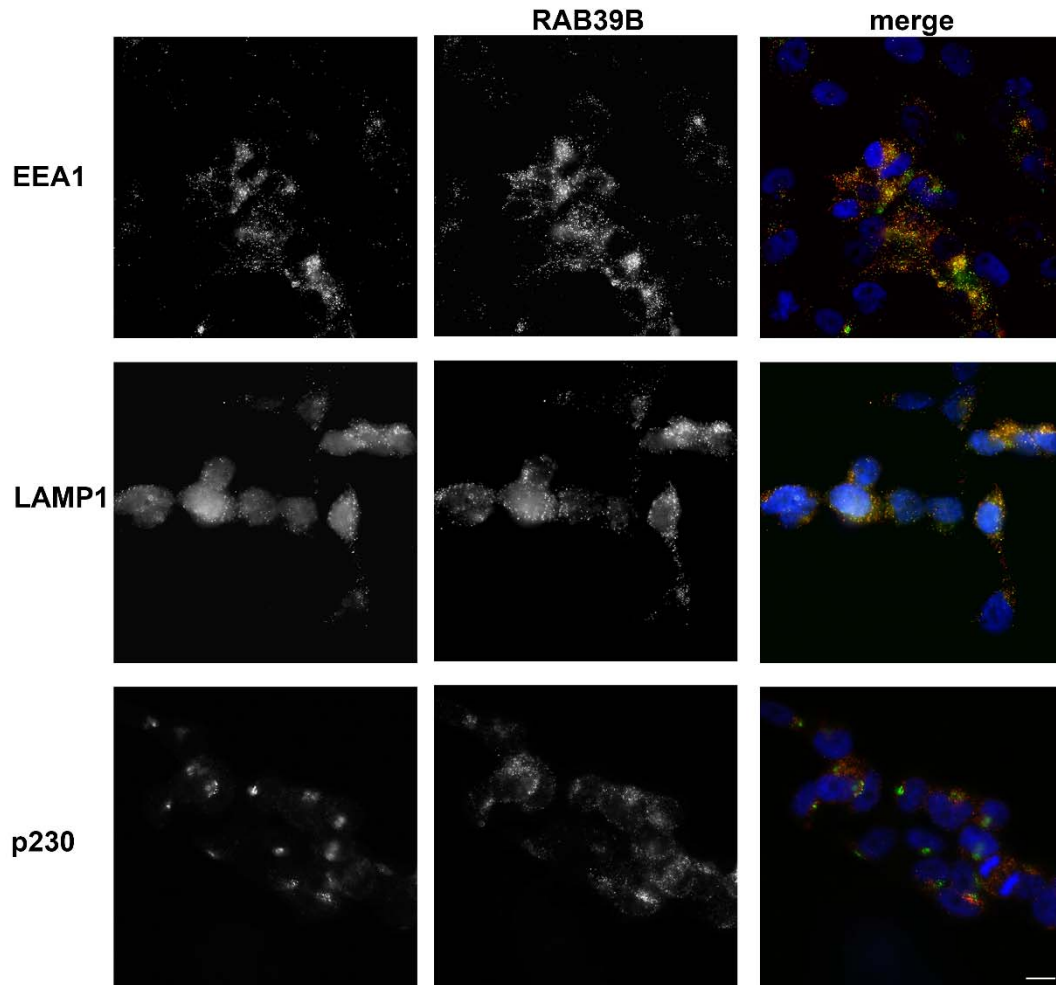


Figure S5: RAB39B co-localizes with markers of the endosomal pathway

The cellular distribution of endogenous RAB39B in BE(2)-M17 neuroblastoma cells was assessed using immunofluorescence co-localization studies. Top panels show co-localization of Early Endosome Antigen 1 (EEA1, green, Santa Cruz Biotechnology Inc, sc-6414, 1:200) with RAB39B (red). The middle panels show co-localization of Lysosomal-associated membrane protein 1 (LAMP1, green, Santa Cruz Biotechnology Inc, sc-80980, 1:200) with RAB39B (red). The bottom panels demonstrate little co-localization of a trans-golgi marker (p230, green, BD Transduction Laboratories, 611280, 1:200) with RAB39B (red). Scale bar 10 μ m.

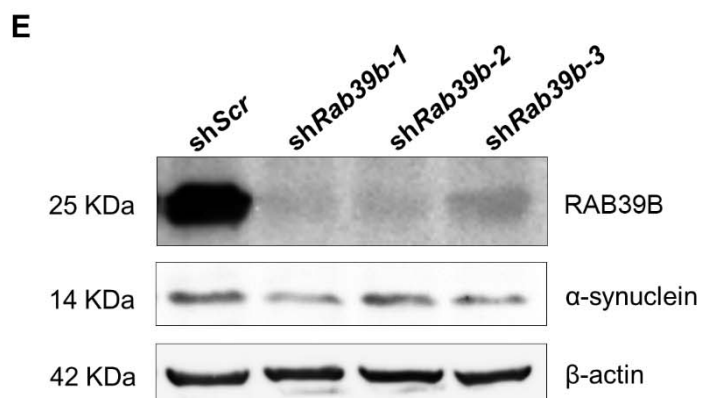
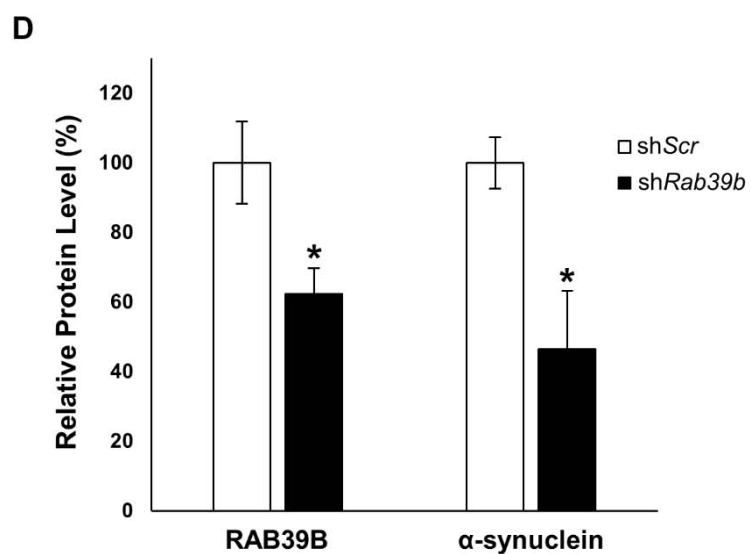
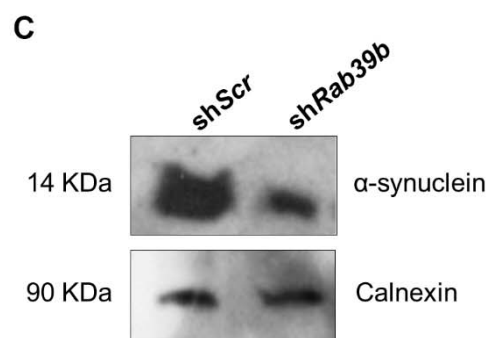
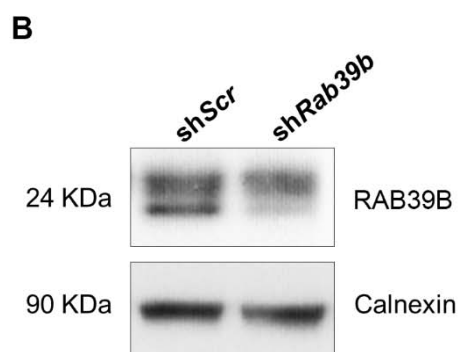
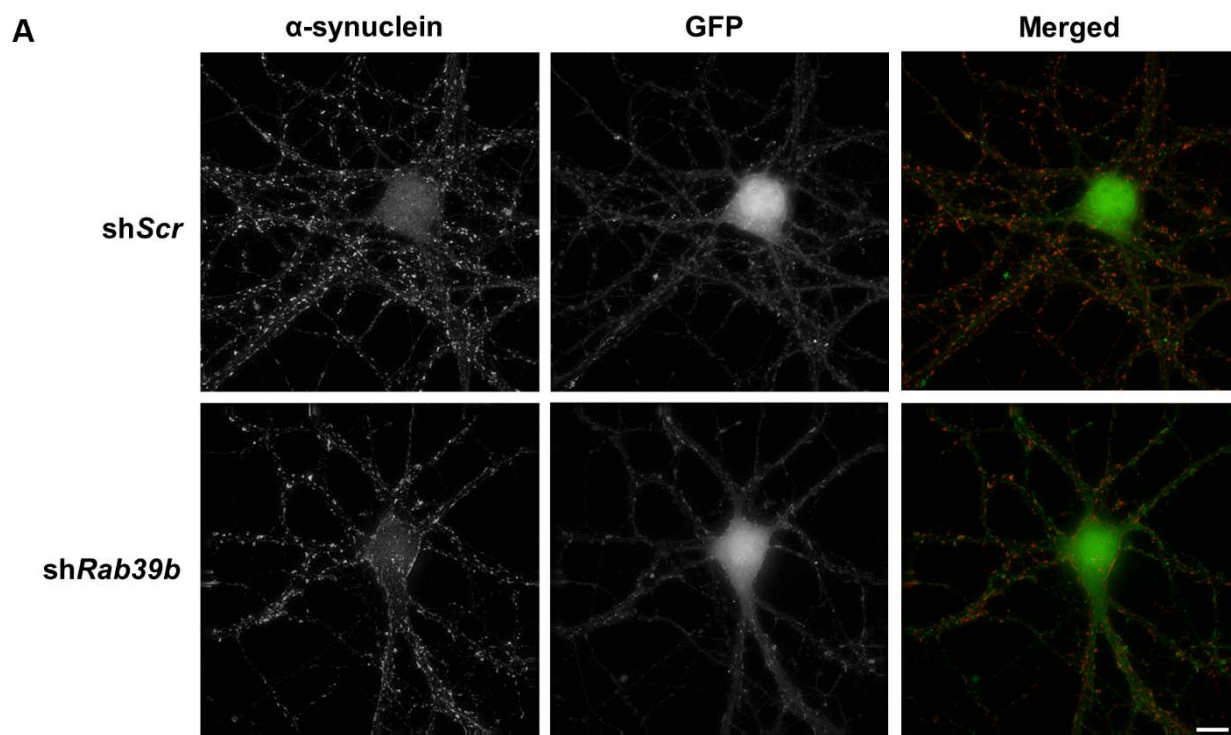


Figure S6: Down regulation of *Rab39b* alters α -synuclein homeostasis

Mouse E18 hippocampal neurons were transduced with lentiviral vectors encoding GFP and either scramble (*shScr*) or *shRab39b* sequences. (A) Robust numbers of α -synuclein immunoreactive puncta were observed in the dendrites of *shScr* control neurons compared to *shRab39b* transduced neurons. Scale bar 10 μ m. (B) Immunoblot of transduced neurons with antibodies directed against RAB39B and calnexin. (C) Immunoblot of transduced neurons with antibodies directed against α -synuclein and calnexin. (D) Quantification of (B) and (C) showed a reduction in the steady state levels of RAB39B and α -synuclein in neurons transduced with *shRab39b* compared to *shScr*. The immunoreactive signals were quantified with a LAS4000 imager and normalized to the loading control calnexin. Protein levels are expressed relative to *shScr* transduced neurons adjusted to 100%. The experiments were performed at least three times. * denotes $P \leq 0.05$. (E) Immunoblot of mouse P19 cells transduced with lentiviral vectors encoding either scramble (*shScr*) or three independent *shRab39b* sequences with antibodies directed against RAB39B, α -synuclein and β -actin. Quantification showed a reduction in the steady state levels of RAB39B ($16 \pm 4.6\%$, mean \pm SEM, $P \leq 0.0005$) and α -synuclein ($53 \pm 3.8\%$, mean \pm SEM, $P \leq 0.005$) in cells transfected with *shRab39b* sequences compared to *shScr*.

Clinical features	Australian Kindred			Wisconsin Kindred	XLMR Families
Previous description	NA	NA	NA	Ref 1,2	Ref 3,4
Person or Pedigree/s	Person II:3	Person II:2	Person II:1	Wisconsin pedigree	D-23 and MRX72 pedigrees
RAB39B mutation	Deletion	Deletion	Deletion	Point mutation	Nonsense/Splice site
Intellectual disability					
Onset Age (*age at clinical evaluation or retrospective assessment)	<2yr	<2yr	<2yr	<2yr	10-52yr (D-23)/Childhood-46yr (MRX72) *
Pregnancy/birth	Normal	Normal	Normal	Normal	Normal
Early motor milestones	Delayed	Normal	Normal	Delayed	Delayed (±)
Speech initiation	Delayed	Delayed	Delayed	Delayed	Delayed (±)
Early learning difficulties	✓	✓	✓	✓	✓ (±)
Intellectual disability	✓	✓	✓	✓	✓
Able to read and write	✗	✓	✓	✓ read (±)	✓ read (±)
Independent living	✗	✗	✗	✓	NR
Behavioral features					
Obsessional behavior	✓	✗	✗	NR	NR
Ritualistic behavior	✓	✗	✗	NR	NR
Hyperactive/disruptive	NR	NR	NR	✓(1/6)	NR
Extrapyramidal symptoms and parkinsonism					
Age at tremor onset	Late childhood	38	44	10-20's	NR
Age at parkinsonism diagnosis	NA	44	45	20's	NR
parkinsonism classification	NA	Akinetic-rigid	Akinetic-rigid	NR	NR
Postural/upper limb tremor	✓	✓	✓	✓(4/6)	NR
Choreoathetosis	✗	✗	✗	✓(1/6)	NR
Shuffling gait	✗	✓	✓	✓(5/6)	NR
Bradykinesia	✗	✓	✓	✓	NR
Dyskinesia	✗	✓	✓	NR	NR
Cogwheel rigidity	✗	✓	✓	✓	NR
L-Dopa response	NA	✓	✓ ^b	✗ (3/3)	NA
Hypokinetic dysarthria	✗	✓	✓	✓	NR
Cerebellar function	Normal	Normal	Normal	Normal	NR
Other					
Autism	✗	✗	✗	NR	✓ (3/12)
Seizures	✗	✗	✗	✓ (2/6)	✓ (3/12)
Macrocephaly	✓	✓	✓	✓	✓
Frontal bossing	✗	✗	✗	✓±	NR
Normal eye examination	✓	✓	✓	✓(4/6)	✓
Strabismus	✗	✗	✗	✓(1/6)	NR
Iris Coloboma	✗	✗	✗	✓ (1/6)	NR
Hydrops	✗	✗	✗	✓(1/6)	NR
Dysmorphism	✗	✗	✗	NR	✗
High arched palate	✗	✗	✗	✓(5/6)	NR
Dementia	✗	✗	✓	NR	NR
Skin depigmented papules	✗	✗	✗	✓4/6	NR
Additional Tests					
MRI	NA	Normal	Abnormal ^c	NA	Normal
Fragile X	Normal	Normal	Normal	Normal	Normal (±)
Karyotype	Normal	Normal	Normal	Normal	NR
CT scan	NA	NA	NA	Megalencephaly	Normal
Copper testing	Normal	Normal	Normal	Normal	NR
Blood count and chemistry	Normal	Normal	Normal	Normal	NR
Urine metabolic testing	Normal ^g	Normal	Normal	Normal	NR
EEG	✗	✗	✗	Abnormal (2/6)	NR
Hearing	Normal	Normal	Normal	Normal	NR

Table S1: Clinical description of the males with mutations in *RAB39B*.

The clinical features of the Australian and Wisconsin kindreds are described in detail. Note that the clinical features of the Wisconsin pedigree are based on the 6 male individuals described previously^{5,6}. Two XLMR pedigrees, D-23 and MRX72, presenting with mental retardation and macrocephaly were described previously^{14,16}.

✓ or ✗ indicates the feature is present or absent in the described individual/pedigree, respectively. In cases where not all of the individuals/pedigrees displayed the trait, the number of affected individuals/pedigrees is defined in brackets. Alternatively, ± indicates the phenotype is present in several individuals or pedigrees but specific number was not defined.

^a Urine test had borderline MPS; ^b side effects to L-Dopa; ^c T2 weighted MRI showed slight bilateral reduction in signal intensity in the substantia nigra and globus pallidus, indicative of iron/calcium deposition. Blood count and chemistry includes: liver function, calcium, uric acid, serum ceruloplasmin/copper/lead/zinc/lipoprotein and parathyroid hormone. NR is not reported. CSF is cerebral spinal fluid; NA is not applicable.

Linkage region 1	Marker	HGSV reference
Beginning	rs17051658	NC_000023.11:g.3624034
End	rs16979497	NC_000023.11:g.14291092
Linkage region 2		
Beginning	rs1174432	NC_000023.11:g.145644895
End	Telomere	NA

GRCh38 assembly, annotation release 106

Table S2: X-chromosome linkage regions identified in the Australian kindred.

Genomic DNA from the mother and 5 offspring of the Australian kindred were genotyped using high density Illumina 610-quad beadchip SNP arrays at the Australian Genome Research Facility. Genotypes were called using the GenCall algorithm implemented in Illumina's BeadStudio package and the likelihood of inbreeding was established using FESim. A subset of ~10,000 SNPs spaced at least 0.15 cM apart were selected for linkage analysis. Parametric linkage analysis using a rare recessive disease model and haplotype reconstruction were performed using MERLIN. Linkage regions were interrogated for CNV (Copy Number Variation) using Genome Studio software and CNV results were filtered with reference to the Database of Genomic Variants (DGV).

Gene	Position (hg19)	Mutation	PolyPhen	SIFT	Sample	CADD score
RAB39B*	X:154490014	Deletion (>19373bp)	NA	NA	II:2	NA
MBNL3	X:131573578	C>G p.Arg21Thr	probably damaging	damaging	II:2	23.90
MAGEA4*	X:151092942	G>A p.Arg269His	benign	NA	II:2	7.36
RAB39B*	X:154490227	G>T p.Thr168Lys	probably damaging	damaging	IV:12	22.60
FANCB	X:14882764	A>G p.Met290Thr	possibly damaging	tolerated	IV:12	10.43
CETN2*	X:151997804	C>T p.Lys60Lys	NA	NA	IV:12	8.94
HEPH	X:65382607	A>G p.Asn13Ser	NA	NA	IV:12	6.00
RBMXL3	X:114426769	A>G p.Asn922Ser	benign	NA	IV:12	5.20
NLGN4X	X:6069437	T>C p.Asn24Ser	benign	tolerated	IV:12	0.01

Table S3: List of novel variants identified by X-exome sequencing in the Australian and Wisconsin kindreds.

X-Exome sequencing and analysis of gDNA by droplet-based multiplex PCR was performed essentially as previously described⁵. Variants identified in individuals II:2 (Australian kindred) and IV:12 (Wisconsin kindred) were filtered against dbSNP138 (<http://www.ncbi.nlm.nih.gov/snp>), 1000Genomes (release20110521), and NHLBI Exome Sequencing Project (ESP6500). Variants were subsequently ranked by potential functional impact using the CADD score⁶. NA = not applicable. *-variants within the haplotype/linkage region. Variants identified in *RAB39B* have been submitted to the NCBI ClinVar database.

Supplemental References

1. Laxova, R., Brown, E.S., Hogan, K., Hecox, K., and Opitz, J.M. (1985). An X-linked recessive basal ganglia disorder with mental retardation. *American journal of medical genetics* 21, 681-689.
2. Gregg, R.G., Metzenberg, A.B., Hogan, K., Sekhon, G., and Laxova, R. (1991). Waisman syndrome, a human X-linked recessive basal ganglia disorder with mental retardation: localization to Xq27.3-qter. *Genomics* 9, 701-706.
3. Giannandrea, M., Bianchi, V., Mignogna, M.L., Sirri, A., Carrabino, S., D'Elia, E., Vecellio, M., Russo, S., Cogliati, F., Larizza, L., et al. (2010). Mutations in the small GTPase gene RAB39B are responsible for X-linked mental retardation associated with autism, epilepsy, and macrocephaly. *American journal of human genetics* 86, 185-195.
4. Russo, S., Cogliati, F., Cavalleri, F., Cassitto, M.G., Giglioli, R., Toniolo, D., Casari, G., and Larizza, L. (2000). Mapping to distal Xq28 of nonspecific X-linked mental retardation MRX72: linkage analysis and clinical findings in a three-generation Sardinian family. *American journal of medical genetics* 94, 376-382.
5. Hu, H., Wrogemann, K., Kalscheuer, V., Tzschach, A., Richard, H., Haas, S.A., Menzel, C., Bienek, M., Froyen, G., Raynaud, M., et al. (2009). Mutation screening in 86 known X-linked mental retardation genes by droplet-based multiplex PCR and massive parallel sequencing. *The HUGO journal* 3, 41-49.
6. Kircher, M., Witten, D.M., Jain, P., O'Roak, B.J., Cooper, G.M., and Shendure, J. (2014). A general framework for estimating the relative pathogenicity of human genetic variants. *Nature genetics* 46, 310-315.